Non-thermal plasma synthesis of plasmonic zirconium nitride nanoparticles

S. Exarhos[1], A. Woodard[2], A. Alvarez[1] and L. Mangolini[1,2]

[1]*Mechanical Engineering Department, Bourns College of Engineering, University of California-Riverside, Riverside, CA, USA*
[2]*Materials Science & Engineering Program, Bourns College of Engineering, University of California-Riverside, Riverside, CA, USA*

Abstract: We present a novel technique for the synthesis of zirconium nitride (ZrN) nanoparticles using a scalable non-thermal plasma process. The system employs a solid zirconium tetrachloride precursor, which is heated at moderately high temperatures to increase its vapor pressure and to deliver it to a non-thermal plasma reactor. Ammonia is used as nitrogen precursor. The synthesized ZrN particles exhibit a plasmon-resonance absorption peak well within the visible spectrum. Depending on the flow rate of ammonia, the absorption peak is controllable from ~640 nm to ~780 nm. XRD and TEM suggest that we synthesize crystalline ZrN particles with a cubic rock salt structure and a fairly monodisperse size distribution centered at ~5 nm. In XRD, we also observe the presence of sharp peaks that may indicate the presence of contaminant ammonium salts, which can form when gaseous ammonia reacts with gaseous $ZrCl_4$. The formation of this contaminant reduces throughput in the system, but the product can be cleaned by annealing or by solvent rinsing. Understanding the processing parameters associated with synthesizing ZrN nanoparticles will allow further study into replacing rare-earth metal plasmonic nanoparticles like gold or silver.

Keywords: Zirconium nitride, plasmon, nanoparticles, non-thermal plasma.

1. Introduction

Localized surface plasmon resonance (LSPR) is a phenomenon that has garnered interest in a variety of fields recently, such as photocatalysis[1], photovoltaics[2], biophotonics[3], spectroscopy[4], sensing[5], and waveguiding[6]. The phenomenon has been observed and well-studied in noble metal nanoparticles, like gold, silver, copper, and platinum[7-9]. Doped semiconducting nanoparticles have also been observed to exhibit LSPR behavior, though not in the visible spectrum.

Luther *et al*. correlate the LSPR frequency with the density of free charge carriers in nanoparticle materials[10], so metals tend to have the highest LSPR frequency, with LSPR peak position well within the visible spectrum. Due to the difficulties with synthesizing pure metallic nanoparticles and the cost associated with noble metals, alternative materials exhibiting plasmonic behavior in the visible spectrum are highly desirable. Group IV transition metal-nitrides have been proposed as potential plasmonic materials to compete specifically with gold-based plasmonic nanomaterials[11,12]. In addition, the ceramic properties of these nitrides allow for high thermal stability[13], and the LSPR frequency can be tuned according to stoichiometry[11].

Our group has previously reported the synthesis of tuneable plasmonic TiN nanoparticles using a nonthermal plasma synthesis technique[14]. These particles exhibit plasmonic behavior with an optimal absorption peak around 790 nm. The peak was shown to be tuneable based on oxide content, with an increased surface oxide associated with red-shifting and diminishing the LSPR peak strength. Replacing the titanium anion with zirconium causes the plasmonic resonance peak to blue shift into the visible spectrum[11,15].

Herein, we outline a scalable non-thermal plasma technique used to synthesize ZrN nanoparticles using anhydrous solid zirconium tetrachloride and ammonia gas as precursors. We show preliminary results that indicate plasmonic behavior from crystalline nanoparticles.

2. Experiment

A schematic of the experiment apparatus is shown in Fig. 1. The system is based on the continuous flow non-thermal plasma reactor described by Mangolini *et al*.[16] In order to synthesize ZrN, we use solid $ZrCl_4$ and gaseous NH_3 as precursors. Solid $ZrCl_4$ has a vapor pressure of ~0.01 torr at room temperature[17], so to increase the concentration of reactants in the system the precursor is heated to 180 ºC in an alumina boat situated near the downstream end of a tube furnace. The flow of the heated argon over the solid precursor provides an estimated $ZrCl_{4,(g)}$ flow rate of ~10 sccm for an argon flow rate of 70 sccm and the aforementioned temperature[17]. It is crucial to inject ammonia into the system as close to the plasma plume as possible, as NH_3 and $ZrCl_{4,(g)}$ will react in the vapor phase to form ammonium salts[18], which are expected to be non-reactive within the plasma.

The plasma reactor is a 2.5 cm OD quartz tube with a thin copper plate wrapped around it as RF electrode. The electrode is ~5 cm in width and the plasma, under optimal conditions, couples to the grounded stainless steel flange downstream of the reaction volume. The RF power

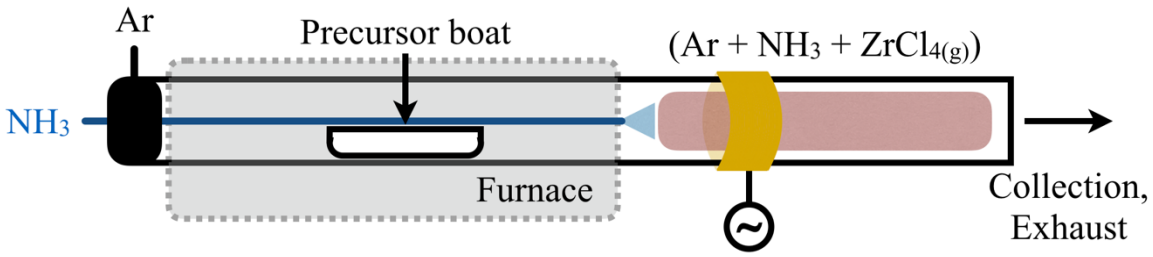

Fig. 1. Schematic diagram of non-thermal plasma apparatus used to synthesize ZrN nanoparticles. Solid $ZrCl_4$ is heated and vaporized under steady flow of argon, and ammonia is introduced to the stream just prior to the plasma plume.

supplied to the electrode is 180 W, which we have found necessary to use in order to synthesize crystalline particles. During particle synthesis, the pressure within the reactor is maintained at 3 torr using a butterfly valve. ZrN particles are collected downstream of the plasma using a stainless steel mesh filter.

Optical absorption measurements have been carried out using a Varian Cary 500 UV/Vis/NIR spectrophotometer with the particles dispersed in a methanol solvent. Diffraction spectra have been generated using a PANalytical Empyrean X-Ray Diffractometer using a CuKα radiation source with a wavelength of 1.54 Å.

3. Results & Discussion

Using the apparatus displayed in Fig. 1 and the methodology listed above, we are able to synthesize crystalline ZrN nanoparticles with an average size of 5 nm. TEM (not shown) confirms the production of highly monodisperse crystalline nanoparticles. The diffraction pattern aligns well with crystalline rock salt-structured ZrN at 33.9º (111), 39.5º (200), and 56.3º (220) (Fig. 2).

In the diffraction spectrum (Fig. 2), we also observe sharp peaks at 32.5º, 46.9º, and 58.1º. We attribute these peaks to ammonium salts that form when NH_3 reacts with $ZrCl_4$ in the vapor phase. Using a simple solvent rinsing process or a low temperature annealing process in inert atmosphere, these contaminating salts can be eliminated. This is demonstrated by Alvarez-Barragan *et al.* with TiN[14].

The produced particles disperse well in methanol, and the color of the dispersion ranges from deep blue/indigo to yellow, depending on the synthesis parameters. We have found that by varying the ammonia flow rate relative to that of argon (and in turn of $ZrCl_4$), we can produce particles throughout this optical range (deep blue/indigo, blue, green, and yellow). UV/Vis/NIR spectroscopy confirms

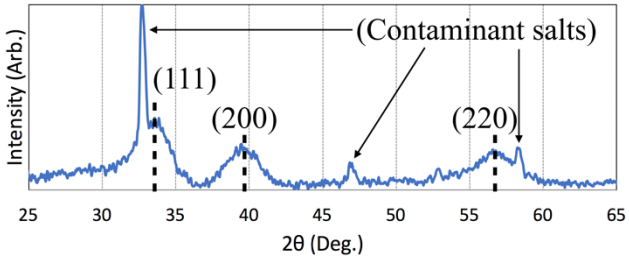

Fig. 2. Normalized diffraction spectrum of synthesized ZrN nanoparticles.

that the absorption peak for these samples correlates with characterization by the naked eye. In Fig. 3, the blue line (peak at 640 nm) corresponds to a sample produced with a low ammonia flow rate that appeared deeply blue, and the green line (peak at 780 nm) corresponds to a sample produced with a high ammonia flow rate that appeared yellow-green.

Alvarez *et al.* observed a similar result in the synthesis of TiN nanoparticles using a similar non-thermal plasma processing technique[14]. Specifically, he noted that both the size and the absorption peak of the produced TiN nanoparticles could be controlled by varying the NH_3 flow rate in the system. Upon further investigation, the group observed that the size of the particles correlated with the amount of oxygen relative to nitrogen – smaller particles had a much higher oxide content, which contributed to a red-shift in the absorption peak. The larger particles more closely approximated the plasmonic behavior associated with TiN with an absorption peak at near 800 nm.

We expect a similar effect in these ZrN particles – they will oxidize at the surface upon exposure to atmosphere. However, preliminary TEM data suggests that we do not produce such a large range of particle sizes. Further experimentation and characterization is required to determine how oxygen may play a role in breadth and position of the absorption peak, but we expect a similar trend in the ZrN as is seen in TiN. Namely, a higher oxide content will lead to a red-shifted and broadened peak[14].

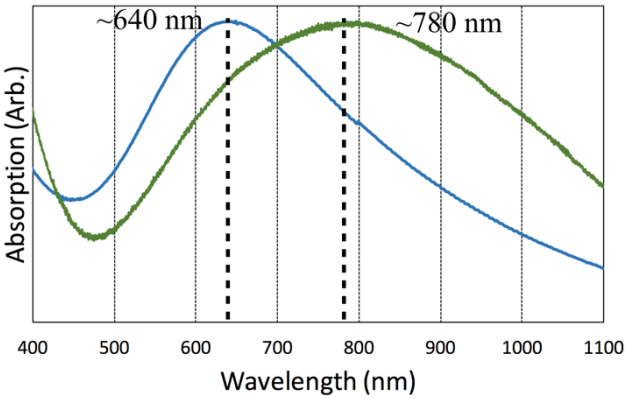

Fig. 3. Normalized absorption spectrum of two different ZrN samples. Sample produced with lower NH_3 flow rate exhibits absorption peak at 640 nm (blue line), sample produced with higher NH_3 flow rate exhibits absorption peak at 780 nm (green line).

This is inferred to be the primary difference between the two samples shown in Fig. 3. If excessive oxidation is observed, the effect can be reduced by alloying silicon into the material system, to act as an "oxygen sink" in the structure[19].

4. Conclusion

We have described a novel technique for the synthesis of plasmonic ZrN nanoparticles using a non-thermal plasma process. Diffraction and TEM characterization show that we produce monodisperse particles with a typical size 5 nm. Further, the particles are crystalline and diffraction peaks align with the cubic ZrN structure. Optical characterization of the produced material suggests a plasmonic effect ranging from ~640 nm to ~780 nm, though further characterization is required to conclude whether we are tuning an absorption peak or we are observing an oxidation effect.

5. References

[1] L.R. Hirsch, Stafford, R.J., *et al*. Proc. Natl. Acad. Sci., **100** (2003), 13549-54.
[2] C. Clavero. Nat. Photon., **8** (2014), 95-103.
[3] M.J. Kale, Avanesian, T., Christopher, P. ACS Catal., **4** (2013), 116-28.
[4] S. Nie, Emory, S.R. Science, **275** (1997), 1102-6.
[5] H. Liao, Nehl, C.L., Hafner, J.H. Nanomedicine., **1** (2006), 201-8.
[6] S. Lal, Link, S., Halas, N.J. Nat. Photon., **1** (2007), 641-8.
[7] M.-C. Daniel, Astruc, D., Chem. Rev., **104** (2004), 293-346.
[8] G.H. Chan, Zhao, J., *et al*. Nano Lett., **7** (2007), 1947-52.
[9] J.J. Mock, Barbic, M., *et al*. J. Chem. Phys., **116** (2002), 6755-59.
[10] J.M. Luther, Jain, P.K., *et al*. Nat. Mater., **10** (2011), 361-6.
[11] G.V. Naik, Kim, J., Boltasseva, A. Opt. Mater. Express, **1** (2011), 1090-9.
[12] A. Lalisse, Tessier, G., *et al*. Sci. Rep., **6** (2016), 38647.
[13] S. Yu, Zeng, Q., *et al*. RSC Adv., **7** (2017), 4697.
[14] A. Alvarez-Barragan, Ilawe, N.V., *et al*. J. Phys. Chem. C, **121** (2017), 2316-22.
[15] A. Reinholdt, Detemple, R., *et al*. Appl. Phys. B, **77** (2003), 681-6.
[16] L. Mangolini, Thimsen, E., Kortshagen, U. Nano Lett., **5** (2005), 655-9.
[17] H. Schäfer, Binnewies, M. Z. Anorg. Allg. Chem., **410** (1974), 251-68.
[18] K.-E. Elers, Saanila, V., *et al*. Chem. Vap. Depos., **8** (2002), 149-53.
[19] Y.-I. Chen, Chang, S.-C., Chang, L.-C. Surf. Coat. Technol., (2017, In press).